SPECTRAL ANALYSIS OF STELLAR JETS: FROM LARGE TO SMALL SCALES.

L. Podio, F. Bacciotti, F. Massi, *INAF-OAA, L.go E. Fermi 5, 50125 Firenze, Italy*, B. Nisini, T. Giannini, S. Antoniucci, *INAF-OAR, Via di Frascati 33, 00040 Monte Porzio Catone, Italy*, P. J. V. Garcia, *CAUP, Rua das Estrelas, P-4150-762 Porto, Portugal*, J. Eislöffel, *Thüringer Landessternwarte Tautenburg, Sternwarte 5, D-07778 Tautenburg, Germany*, T. P. Ray, *School of Cosmic Physics, DIAS, 5 Merrion Square, Dublin 2, Ireland*, C. Dougados, *LAOG, BP 53, F-38041 Grenoble Cédex 9, France*, M. Takami, *Subaru Telescope, National Astronomical Observatory of Japan, 650 North A'ohoku Place, Hilo, HI 96720, USA.*

Stellar jets play a key role in the overall star formation process. The ejection of these flows, in fact, is deeply connected with the accretion process and they can be responsible for the removal of the excess angular momentum from the disk, thus allowing the material to accrete from it onto the star. To confirm this picture and to constrain the launching mechanism we studied the structure of stellar jets both over large scales (Sect. 1) and near the source (Sect. 2) where the acceleration and collimation processes take place.

1. LARGE SCALE PHYSICAL/DYNAMICAL JET STRUCTURE

Optical/NIR diagnostics To derive the conditions of the plasma along a sample of HH jets we developed a combined optical-infrared diagnostics, applied to moderate spatial/spectral resolution data taken with 3.6m-EFOSC2 and NTT-SOFI ([7], [8]). From the flux ratios of the emission lines in the range 0.6-2.5 μm we derived important parameters such as the visual extinction, the electron and total density (n_e, n_H), the ionization fraction (x_e) and the temperature (T_e). The main advantage of this approach is that the optical/NIR range comprises transitions from many atomic and molecular species which have different excitation temperatures and critical densities, thus allowing us to probe the density and temperature stratification behind each shock front along the beam.

The jet physical structure The potential of our spectral diagnostics is evident in Fig. 1 which shows the variation of the physical parameters along the HH 34 jet. The values of n_e and T_e derived from the [Fe II] lines ([6]), in fact, trace a component of the post-shocked gas which is denser and cooler ($n_e \sim$ 1-5 10^3 cm^{-3}, $T_e < 10^4$ K) with respect to that traced by the optical [S II], [N II] and [O I] lines ([1], $n_e \sim$ 0.1-3.4 10^3 cm^{-3}, $T_e \sim$1-2 10^4 K) . An important parameter is the ionisation fraction. The estimated values demonstrate that the gas in the jet is only partially ionised ($x_e \sim$0.03-0.3), thus the total density is of ~0.1-3 10^4 cm^{-3}. Even denser layers of the post-shocked gas (n_e up to 10^6 cm^{-3}) have been traced through [Fe II]λ7155/λ8617 and Ca IIλ8540/[Ca II]λ7290 ratios. A similar density and temperature stratification was found also along the HH 1 and HH 111 jets ([7], [8]).

The jet dynamics From the physical parameters derived through the diagnostics, following the procedures explained in [7], [8], we estimated the mass flux rate ($\dot{M}_{jet}$) transported by the jet. This is a fundamental quantity governing the jet dynamics and which enters all comparisons between observations and theoretical magneto-hydro dynamic (MHD) models

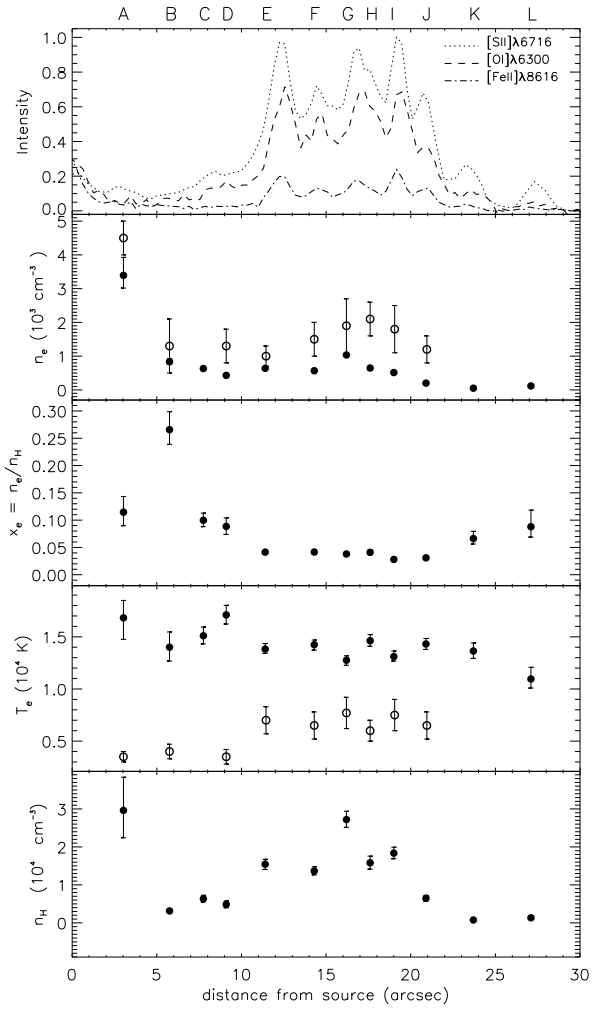

Figure 1: Variation of the derived physical parameters along the HH 34 jet. The open circles are the values derived from the [Fe II] lines ([6]), while the filled circles are parameters inferred from the optical S^+, N^+ and O^0 lines using the BE technique ([1]). The zero point of the spatial scale is the driving source HH 34 IRS.

(in the models $\dot{M}_{jet}/\dot{M}_{acc} \sim 0.01 - 0.1$, where $\dot{M}_{acc}$ is the mass accretion rate [5], [9]). For our sample of jets we obtained $\dot{M}_{jet} \sim 5\ 10^{-8}$ M$_\odot$ yr^{-1}. From the $\dot{M}_{jet}$ value we derived an estimate of the flux of linear momentum $\dot{P}_{jet} \sim 10^{-5}$ M$_\odot$ yr^{-1} km s^{-1}, which is higher or comparable to the one measured for the surrounding molecular flows suggesting that the latter can be jet driven.

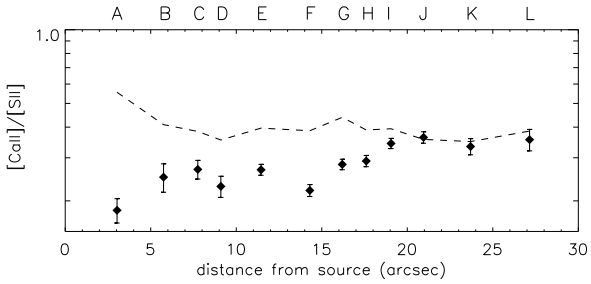

Figure 2: The discrepancy between observed (diamonds) and predicted (dashed line) [Ca II]/[S II] ratios indicates a depletion of Ca of ∼50% in the innermost knots of the HH 34 jet.

Dust grains in jets Refractory species, such as Calcium, are often depleted in the interstellar medium because their atoms are locked onto dust grains. On the other hand, the passage of shocks can destroy the dust releasing the refractory atoms into the gas cloud ([2], [4]). Thus an estimate of the depletion of refractory species can be used to gauge the amount of dust grains in the jet beams.

To this aim we compared observed and expected ratios between emission lines of refractory and non-refractory species. The expected ones are calculated through the derived parameters and assuming solar abundances ([7], [8]). Fig. 2 shows that along the HH 34 jet Calcium is depleted up to 50%. Thus the shocks occurring along the jet beam (v_s ∼20-40 km s^{-1}) are not strong enough to completely destroy the dust grains.

Interestingly, the depletion of Calcium tends to decrease with the distance from the source. This can only be explained if the dust in the beam comes from the disk and is gradually destroyed by the working surfaces as they propagate outwards. Note that we are not observing ambient dust since it is easily destroyed by the passage of the leading bow-shock which has large shock velocity (100-400 km s^{-1}) and the dust reformation timescale is much larger than the dynamical time of the jet (10^3 - 10^4 yr). This finding can put severe constraints on the size of the disk region from which the jet is launched thus allowing to test the validity of the MHD models proposed to explain the jet origin ([5], [9]).

2. TOWARD THE JET BASE: ACCRETION VS EJECTION

Spectro-astrometry To unveil the jet engine and the nature of the accretion-ejection relationship one has to study the jet base. Observations are hampered by the maximum angular resolution that can be achieved with modern instrumentation (∼0.″7, i.e. 100 AU in the nearest star forming regions at ∼140 pc, in seeing-limited conditions; ∼0.″1, i.e. 14 AU, with Adaptive Optics systems). A novel technique to explore the circumstellar region down to few mas (i.e. fractions of AU) is the so called spectro-astrometry (SA). Through SA one can constrain the emission line region thus allowing us to detect the microjets emission over the star continuum and to disentangle inflowing and outflowing contributions in the line profiles. The technique consists in measuring the centroid of the emission as a function of the wavelength. In this way if the emission comes from a spatially unresolved extended wind with distinctive features in its spectrum, a shift of the centroid with respect to the star continuum is expected at the wavelength of the feature ([10]).

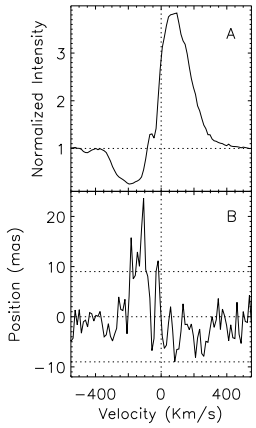

Figure 3: Spectro-astrometric analysis of the RU Lupi HeI line. The line profile (A) and the spectro-astrometric signal (B) are shown. The horizontal lines in panel B indicate the star continuum $\pm 3\sigma$ level. The plot shows the presence of an extended emission in the HeI line.

The origin of permitted He and H lines While forbidden emission lines are associated to the jet, permitted lines are thought to be excited in the accreting gas. Nevertheless, some recent works showed that they can include a contribution from the wind ([3]). Observational confirmations of this hypothesis can give useful hints to the development of models of the complex star-disk region. To this aim we investigated the origin of H and He permitted lines through ISAAC/NACO spectra of the T Tauri star RU Lupi. Interestingly, the SA analysis of the HeI 10830 Å line shows an extended emission superimposed to the absorption feature due to a spherical inner wind (see Fig. 3). Thus to model this line it is necessary to consider not only the emission from the accretion columns but, also, the contributions from spherical outflowing gas and from a collimated extended wind. Through SA we analysed also the Paschen and Brackett H emission lines detected over the RU Lupi continuum emission. In this case, however, no SA signal was detected. Therefore, if there is a wind contribution to the H lines this comes from a region <1 AU which is the accuracy of the SA analysis.

References: [1] Bacciotti, F., Eislöffel, J. 1999, A&A, 342, 717. [2] Draine, B. T. 2003, astro-ph/0304488. [3] Edwards, S., Fischer W., Hillenbrand, L., Kwan, J. 2006, ApJ, 646, 319. [4] Jones, A. P. 2000, JGR, 105, 10257. [5] Königl, A. & Pudritz, R. E. 2000, PPIV, 759. [6] Nisini, B., Caratti o Garatti, A., Giannini, T., Lorenzetti, D. 2002, A&A, 393, 1035. [7] Nisini, B., Bacciotti, F., Giannini, T. et al. 2005, A&A, 441, 159. [8] Podio, L., Bacciotti, F., Nisini, B. et al. 2006, A&A, 456, 189. [9] Shu, F. H., Najita, J.R., Shang H. & Li, Z.-Y. 2000, PPIV, 789. [10] Whelan, E. T., Ray, T. P., Bacciotti, F. et al. 2005, Nature, 435, 652.